UCSF
UC San Francisco Previously Published Works

Title
The Effects of Aging on Apoptosis Following Myocardial Infarction

Permalink
https://escholarship.org/uc/item/4cz7v854

Journal
Cardiovascular Therapeutics, 31(6)

ISSN
1755-5914

Authors
Boyle, Andrew J
Hwang, Joy
Ye, Jianqin
et al.

Publication Date
2013-12-01

DOI
10.1111/1755-5922.12043

Peer reviewed

eScholarship.org Powered by the California Digital Library
University of California

NIH Public Access
Author Manuscript
Cardiovasc Ther. Author manuscript; available in PMC 2014 December 01.

Published in final edited form as:
Cardiovasc Ther. 2013 December ; 31(6): e102–e110. doi:10.1111/1755-5922.12043.

The Effects of Aging on Apoptosis Following Myocardial Infarction

Andrew J Boyle[1,2], **Joy Hwang**[1], **Jianqin Ye**[1,2], **Henry Shih**[1], **Kristine Jun**[1], **Yan Zhang**[1], **Qizhi Fang**[1,2], **Richard Sievers**[1], **Yerem Yeghiazarians**[1,2], and **Randall J Lee**[1,2,3]

[1]Department of Medicine, Division of Cardiology, University of California San Francisco, San Francisco CA

[2]Edyth and Eli Broad Center for Regenerative Medicine and Stem Cell Research, University of California San Francisco, San Francisco CA

[3]Cardiovascular Research Institute, University of California San Francisco, San Francisco CA

Abstract

Background—Aging is associated with higher incidence of heart failure and death following myocardial infarction (MI). The molecular and cellular changes that lead to these worse outcomes are not known.

Methods and Results—Young and aging mice underwent induction of MI by LAD ligation. There was a significant increase in mortality in the aging mice. Neither the young nor aging hearts after MI had inducible ventricular tachycardia. Cardiomyocyte apoptosis increases early after MI in young and aging mice, but to a much greater degree in the aging mice. Caspase inhibition with Ac-DEVD-CHO resulted in a 61% reduction in activated caspase 3 and an 84% reduction in apoptosis in cardiomyocytes in young mice ($p<0.05$), but not in aging mice. Gene pathway profiling demonstrated activation of both the caspase and Map3k1/Mapk10 pathways in aging mice following MI, which may contribute to their resistance to caspase inhibition.

Conclusions—Aging hearts activate distinct apoptotic pathways, have more cardiomyocyte apoptosis, and are resistant to anti-apoptotic therapies following MI. Novel or combination approaches may be required to improve outcomes in aging patients following MI.

Keywords

apoptosis; aging; ventricular remodeling; heart failure; cardiomyocyte

Introduction

Aging is associated with a higher incidence of myocardial infarction (MI) (1). Older patients are not only more likely to suffer an MI, but are more likely to develop heart failure (2) or die (3) as a consequence. The cellular and molecular reasons for the dramatically worse outcomes in the aging population remain incompletely understood (4).

Myocardial infarction causes massive cell death in the infarct zone and this damaged tissue is replaced by scar, resulting in impaired contractile function of the left ventricle. After this initial insult, there is ongoing loss of cardiomyocytes at the edge of the infarcted tissue (border zone) via the process of apoptosis. This continued loss of cardiomyocytes

Address for Correspondence: Andrew Boyle MBBS, PhD, Associate Professor of Medicine, University of California San Francisco, 505 Parnassus Ave, Box 0103, San Francisco CA 94143, Phone 415-353-3817. Fax 415-353-3090, andrewboyle500@gmail.com.

NIH-PA Author Manuscript
NIH-PA Author Manuscript
NIH-PA Author Manuscript

NIH-PA Author Manuscript

NIH-PA Author Manuscript

NIH-PA Author Manuscript

contributes to infarct expansion and ventricular dilation, the hallmarks of post-infarction remodeling. Aging has been associated with higher levels of apoptosis following MI (5,6) but the molecular underpinnings of this increase in apoptosis are incompletely understood.

We have previously studied the aging murine heart and demonstrated that the age-related decline in cardiac function is associated with parallel increases in both pro-and anti-apoptotic factors. These opposing influences balance each other out, resulting in no overall change in the number of apoptotic cardiomyocytes (7). Importantly, we found that this occurred by age 18 months, and was not restricted to the very elderly, senescent mouse. Although much is known about apoptosis following MI in young animals, little is known about the apoptotic pathways in the aging heart after MI. Are compensatory anti-apoptotic mechanisms invoked after MI, as is seen in the non-infarcted aging heart? We therefore studied aging hearts following MI to determine the effects of aging on apoptosis after MI, and to assess the response to anti-apoptotic therapies.

Experimental Procedures

Animals were handled according to the guidelines of the Institutional Animal Care and Use Committee of the University of California, San Francisco, who specifically approved this study. Young mice were 3 months, aging were 18 months of age, as previously characterized by our group (7). Male C57BL/6J mice were used for all studies.

Myocardial Infarction

MI was induced surgically by a permanent ligation of the left anterior descending (LAD) coronary artery as we have previously described (8,9). Briefly, with the animal anesthetized and ventilated, permanent ligation of the LAD is made by a 7-0 suture in the anterior myocardium at 50% of the length of the heart from the anterior-inferior edge of the left atrium to the apex. The chest is then closed and the animal allowed to recover.

Echocardiography

Echocardiograms were obtained at baseline, 2 days post-MI, and at day 28 post-MI; left ventricular (LV) volumes (end-systolic (ESV) and end-diastolic (EDV) volumes) were measured as previously described (7,8). Analyses of the echocardiography images were performed by an investigator who was blinded to the identity of the treatment groups. LV ejection fraction was calculated as

$$LVEF = [(LVEDV - LVESV)/LVEDV] \times 100$$

Electrophysiology Studies

Mice (n=3 young and n=3 aging) at day 3 after MI were anesthetized, intubated, and the chest cavity exposed and retracted. Peripheral recording electrodes were placed into the skin. Bipolar stimulation electrodes were lowered directly on to the right ventricle by direct visualization. A multiple channel Bloom cardiac stimulator (Fischer Medical Technologies, Inc., Broomfield, CO) was used. Stimulation thresholds were assessed by increasing the stimulation output (milliamps — mA) to a point of consistent ventricular capture. This level was confirmed by beginning at high output and decreasing until loss of ventricular capture. With a margin for safety, the typical stimulation output used was 2–5 mA. Basic drive cycle lengths were 100–120 ms for a pacing train of 8–10 beats, and the ventricular effective refractory period (VERP) was assessed for each mouse. Once these basic data were obtained, a ventricular stimulation protocol was used to determine whether the mice exhibited inducible monomorphic ventricular tachycardia. Double and triple extrastimuli were given until the tightest intervals achieved or until ventricular tachycardia was induced.

NIH-PA Author Manuscript

NIH-PA Author Manuscript

NIH-PA Author Manuscript

Testing was repeated for multiple trials in order to verify the reproducibility of results. Following ventricular stimulation protocols, each mouse was sacrificed.

Tissue preparation and analysis

In the first study, animals were sacrificed at day 28 post-MI under general anesthesia. Hearts were arrested in diastole with injection of concentrated KCl and the hearts removed (n=6 young, n=6 aging) and perfused with 10% neutral buffered formalin via the ascending aorta and then paraffin embedded. Sections from the mid-ventricular level were examined for fibrosis using Masson's trichrome staining. Quantification of fibrous tissue was performed on photomicrographs and quantified by using ImagePro (Media Cybernetics Inc, Bethesda, MD) software.

Infarct size

Scar size was analyzed at the mid-papillary level by an investigator who was blinded to the identity of the sections. The percent scar within the infarct zone was determined by manually tracing the areas of interest and measured automatically by the computer. IZ was defined as an area continuously enclosed by scar spanning >50% of the wall thickness. The area of the tissue staining blue was then traced manually and the percentage of the total area of interest occupied by scar was obtained. To assess the circumferential extent of the infarct, the epicardial and endocardial infarct lengths and epicardial and endocardial circumferences were traced manually using ImagePro Plus. Epicardial infarct ratio was obtained by dividing the epicardial infarct length by the epicardial circumference. Endocardial infarct ratio was calculated similarly. The circumferential extent of the infarct was calculated as [(epicardial infarct ratio + endocardial infarct ratio)/2] × 100, as previously described (9).

Measurement of Vascularity

In order to assess vascularity, sections were stained for the vascular markers CD31 and alpha smooth muscle actin. Sections were de-paraffinized, rinsed, and treated with a universal block (Rodent Block M, Biocare) for 30 minutes. A primary rat antibody against CD31 (Biocare, 1:50) was applied to the sections for 2 hours at room temperature. A Rat Detection Kit (Biocare) was used to detect the rat anti-CD31 antibody. The stain was developed using DAB (Biocare). Sections were again blocked using Rodent Block M, and then stained using a mouse primary antibody against alpha-smooth muscle actin (SMA) (Sigma-Aldrich, St. Louis, MO; 1:200 dilution in TBS) for one hour, and a Mouse on Mouse Polymer (Biocare) conjugated to alkaline phosphatase was applied to the sections for 20 minutes at room temperature. The stain was developed using a Ferangi Blue Chromogen Kit (Biocare). Low power (4×) photomicrographs were taken of three regions: IZ, BZ and RZ. ImagePro Plus 6.0 software was used to select brown CD31+ staining after manually selecting the region of interest and the vessel area density was obtained automatically for each of the three regions. Additionally, the number of vessels staining positive for alpha SMA per high power field (HPF) were counted within each region.

Cardiomyocyte Apoptosis Early After MI

In a second study, a separate group of male C57Bl6 mice underwent creation of MI by LAD ligation as described above (n=9 young and n=9 aging). Instead of surviving them to 28 days, we focused this study on the early time-point day 3 after MI, in order to define factors that may account for the excess mortality in the MI survival study. At day 3 after MI, mice were humanely sacrificed as described above and the hearts were removed. In a subset of mice (n=3 young and n=3 aging), the hearts were immediately cut into geographic regions: infarct zone (IZ), border zone (BZ) and remote zone (RZ). These regions were rapidly frozen separately in liquid N2 and were used for RNA analysis. In the remainder, the hearts

NIH-PA Author Manuscript

NIH-PA Author Manuscript

NIH-PA Author Manuscript

were perfused with 10% NBF via the ascending aorta and the hearts were paraffin embedded for immunohistochemistry (n=6 young, n=6 aging).

Histology and Immunohistochemistry

Apoptosis of cardiomyocytes was detected by the co-localization of antibody staining for cardiac troponin-I (Abcam, Cambridge, MA) and TUNEL staining (ApopTag; Chemicon, Temecula, CA) within the same cell as previously described.(7) Apoptotic CMs were quantified by blinded reviewers counting the number of positive cells within each high power field. Activation of caspase-3 in cardiomyocytes was detected by the co-localization of antibody staining for activated caspase-3 (BD Pharmingen, San Jose, CA) and for cardiac troponin-I within the same cell. The percent of the troponin-I positive area that was also positive for caspase-3 was quantified using ImagePro software. Caspase independent cardiomyocyte apoptosis was quantified by co-staining troponin-I with AIF: 1:50 (Cell Signaling). The baseline non-infarcted control tissues used for the experiment were derived from animals used in a prior experiment (7) to minimize use of aging animals.

RNA analysis

Total RNA was isolated from separate areas of the left ventricles: the infarct zone, border zone and remote zone (IZ, BZ, RZ) of young (n=3) and aging (n=3) mice by TRIzol reagent (Invitrogen). Trace genomic DNA in total RNA was removed by DNase I and RNeasy Mini Kit (Qiagen). cDNA was generated from 1 ug of total RNA by using SuperScript III First-Strand Synthesis kit (Invitrogen). Microarrays were performed using Affymetrix 1.0 Mouse gene chip. To minimize the number of mice used, we used the RNA extracted from young (n=3) and aging (n=3) mice from our prior study as baseline. Importantly, although we used RNA from the same animals, we used different samples of this RNA and the microarray analysis was repeated for this experiment, to avoid a potential batch effect. The results were very consistent with the prior data (7) which strengthens our data. Data were normalized using robust multi-array average (RMA) method. Control and low performing probesets (those with intensity values below a threshold across all samples, the threshold was taken to be the global lowest 25th percentile of intensity values) were excluded from analysis. Also, based on Affymetrix's annotation information, only those probesets which were part of the main design of the array and perfectly matching only one sequence were considered for analysis of differential expression. 20648 out of 35557 probesets remained after filtering. Biological pathway analysis was performed using the GenMAPP CS application for Mac, which is freely available at http://www.genmapp.org/. This allows the data derived from the microarrays to be placed into a meaningful biological context and analyzed in that way, rather than as single genes. We performed Gene Ontology (GO) Elite analysis for overrepresentation of genes in different regions of the heart in young and aging mice using the GenMAPP platform. The data listed in Supplemental Tables 1 and 2 represent the results of the GO-Elite analysis of which pathways were overrepresented. Figure 2D demonstrates how GenMAPP can take a statistically positive gene set and display it in a biologically understandable format (10,11).

Caspase Inhibition Study

In a third separate study, we attempted to define if inhibition of activated caspase-3 could reduce the early apoptosis of cardiomyocytes following MI. Another group of male C57Bl6 mice (n=6 young, n=6 aging) underwent LAD ligation to induce MI. Each animal received the caspase inhibitor Ac-DEVD-CHO 3mg/kg via intraperitoneal injection daily starting on the day of MI and continuing until day 3 post-MI. The animals were then euthanized and the hearts harvested, formalin fixed, paraffin embedded and analyzed for the amount of cardiomyocyte caspase-3 activation and apoptosis, as described above. The results were compared to animals in study 2.

NIH-PA Author Manuscript

NIH-PA Author Manuscript

NIH-PA Author Manuscript

Statistical analysis

Data are presented as mean± SD unless otherwise stated. Continuous data were compared between young and aging using unpaired Student's t-test and categorical variables using Chi-square test. Timecourse echocardiography data was analyzed within groups using ANOVA with Fisher's post hoc test. Microarrays were normalized for array-specific effects using Affymetrix's "Robust Multi-Array" (RMA) normalization. For statistical analyses, we removed all array probesets where no experimental groups had an average log2 intensity greater than 3.0. This is a standard cutoff, below which expression is indistinguishable from background noise. Linear models were fitted for each gene using the Bioconductor "limma" package in R (12,13). Gene expression changes were integrated with gene sets and biological pathways using gene map annotator and pathway profiler (GenMAPP 2.0) (10,11).

Results

Age-dependent Increase in Mortality Following MI

In order to define the appropriate age in which to study "aging", we performed LAD ligation to create myocardial infarction in mice of different ages. At 18 months of age, there is a decline in survival to approximately 50% following MI. At 21 months of age, no animals survive MI (p=0.005, see Online Supplemental Figure 1). We therefore used 18-month old mice for the "aging" comparator in the rest of our experiments, because, at this age, there was a demonstrable reduction in survival (Figure 1), yet enough mice survived to be able to be studied. Serial echocardiography provided insight into the remodeling process. Aging mice had larger left ventricular volumes at baseline and a lower left ventricular ejection fraction. Over 28 days, the young animals' ventricles dilated to a greater degree than the older animals. There was a significant increase in heart weight in the young but not in the aging, resulting in similar end-diastolic and end-systolic volumes at day 28 (Table 1 and Figure 1). As a result of the greater remodeling in the young MI survivors, LVEF was no longer significantly different between groups at day 28.

No Difference in Infarct Size, Arrhythmia Inducibility or Blood Vessel Density With Age

We analyzed the size of the infarct scar in the young and aging 18 month-old mice. Of those animals that survived to day 28, infarct size was not different between young and aging mice (Figure 2). Electrophysiological studies were performed to assess ventricular effective refractory period and inducibility of ventricular tachycardia (VT) on young and aging mice after MI. As was shown in our previously published data in young and aging mice at baseline (7), there was no difference in VERP or inducibility of VT between age groups after MI. In addition, there is no difference in capillary density or number of arterioles in aging animals compared to young animals (Figure 2).

Cardiomyocyte Apoptosis Increases Post-MI via Caspase-Dependent and Caspase-Independent Mechanisms

Because the excess mortality in aging mice was seen *early* post-MI (Figure 1), we repeated the experiment and studied the gene and protein expression in the left ventricle at day 3 post-MI, to assess for pathological changes that may contribute to this excess early mortality. We used immunohistochemistry and immunofluorescence techniques to specifically identify changes occurring in cardiomyocytes and not in other cell types. More apoptotic TUNEL positive cardiomyocytes are seen following MI in both young and aging mice compared to baseline. This is due to an increase in both caspase-dependent and caspase-independent apoptosis. The number of caspase-3 positive cardiomyocytes increases following MI in both the young and aging mice (Figure 3). Following MI, the gene

NIH-PA Author Manuscript

NIH-PA Author Manuscript

NIH-PA Author Manuscript

expression profile changes significantly, both in young and aging mice (see online supplement table 1). Many biological pathways were differentially regulated in aging compared to young mice after MI. Using GenMAPP, a pathway analysis tool to assess changes in the entire biological pathway, rather than individual genes, we studied pro- and anti-apoptotic pathway expression. Both young and aging mice demonstrated upregulation of some pro-apoptotic and some anti-apoptotic genes and gene pathways. In the aging mice, however, we discovered two separate upregulated apoptosis gene pathways following MI, which were not evident in young mice. There was upregulation of caspases 3 and 7 (caspase-dependent apoptosis), as well as upregulation of the Map3k1/MapK10 pathway of apoptosis (caspase-independent apoptosis) (see figure 4). Both the increased caspase proteins, as well as the Map3k1/MapK10 pathway, which is previously undescribed in the aging mouse heart, may contribute to excess cardiomyocyte apoptosis seen in aging hearts following MI.

Caspase Inhibition Alone Following MI is Effective in Young Mice, But Not in Aging Mice

To determine the effects of apoptosis inhibition on cardiomyocyte apoptosis early after MI, we used a caspase inhibitor Ac-DEVD-CHO administered at the time of MI and for 3 days after. This resulted in a 61% reduction in activated caspase-3 expression in cardiomyocytes ($p<0.05$), and an 84% reduction in cardiomyocyte apoptosis in the young animals ($p<0.05$, see figure 4). However, in the aging mice, caspase inhibition had no effect on activated caspase-3 expression (−13%, p=ns) or cardiomyocyte apoptosis (−30%, p=ns) (Figure 3).

Discussion

This series of experiments has several important findings. First, MI is associated with higher mortality in aging mice, and that does not appear to be due to increased susceptibility to arrhythmia. Second, there is evidence of excess cardiomyocyte apoptosis in response to MI in aging hearts. Third, we show that cardiomyocyte apoptosis is mediated by different pathways in aging hearts compared to young hearts.

As expected, we found an age-dependent increase in mortality following MI. However, we found no difference in infarct size between the young and aging mice that survived to 28 days. Some prior studies have found that aging animals have larger infarcts than young animals (14,15), whereas other studies have shown no difference (6,16). The reason for these discrepancies is not completely clear. There is likely to be a gradation of the remodeling process in aging, with very elderly senescent mice suffering greater degrees of remodeling than less elderly mice. In captivity, the life expectancy of C57/Bl6 is approximately 30 months (17), therefore our aging mice, at 18 months of age, are not senescent as used by some other laboratories. Many factors influence how the age on one species relate to the age on another. These include the life expectancy, duration of fertility, development of cancers, genetic heterogeneity, diet and lifestyle, disease states and potentially many other factors. Taking all this into account, with a captivity life expectancy of 30 months for C57/Bl6 mice, one can try to extrapolate to humans. But what is human life expectancy? Is it 45 years as it was in the 19th century without sanitary and medical interventions? Or is it over 80 years as it is now in much of the western world? This suggests our use of 18-month-old mice would be somewhat equivalent to middle age in humans. Jugdutt and colleagues calculate that one mouse year = 34–38 human years (18).

One possible explanation for the lack of difference between aging and young mice infarct size is that mice age at different rates, just as people do. The high early mortality may have been associated with larger infarcts in mice behaving more like the very elderly, and the aging mice that survived may have been phenotypically more like young mice – the “survivor effect”. To avoid this confounding interpretation of data analyzed from the later

NIH-PA Author Manuscript

NIH-PA Author Manuscript

NIH-PA Author Manuscript

time-point, we focused our tissue and gene studies on an early time-point, day 3, so we would include mice that may have died.

Most animal studies of myocardial infarction and left ventricular remodeling are performed in young animal models. However, MI is a disease of aging adults. Studies in the aging heart are imperative if we are to understand how the aging heart responds to myocardial infarction, and how this response differs from young hearts. We show that the expression of caspase-3 is increased after MI in both young and aging mice, but the increase is greater in the aging mice. Other laboratories have also demonstrated increased cardiomyocyte apoptosis following MI with aging. Liu and colleagues demonstrated an increase in cardiomyocyte apoptosis in aged rats following ischemia-reperfusion injury, which was associated with an increase in Bax:Bcl-2 ratio (5). Our studies are congruent with theirs by showing differences in gene profiles between young and aging animals after MI. However, our results differ from theirs in that we did not show an increase in these same apoptotic genes. This may be due to species differences between rats and mice. In another study, Lehrke and colleagues (6) showed that aging rats had more apoptotic cardiomyocytes following MI than young rats. More importantly, they showed that aging rats are able to respond to treatments that reduce cardiomyocyte apoptosis, however the response to treatment was less marked in the aging rats. Taking their data together with ours, one could reasonably speculate that the activation of multiple pathways toward apoptosis in the aging heart after MI contributes to the observed inefficacy of treating a single apoptosis pathway in aging mice.

Prevention of cardiomyocyte apoptosis is a mechanism that is consistently observed with regenerative therapies following myocardial infarction (8,19–23). Herein we show a greater burden of apoptosis in ageing hearts after MI. Previously we have shown that cell therapy acts via stimulating resident cardiac progenitor cells (CPCs) to reduce cardiomyocyte apoptosis (22), and that aging CPCs have a significant reduction in numbers and impairment in proliferative capacity (24). Taken together, these factors may at least partly explain the disappointing results of clinical trials of cell therapy in aging patients after MI. Future studies addressing post-infarction CPC therapy in elderly patients should take into account the increased burden of apoptosis, as well as the reduced number and function of aging CPCs.

Our study highlights the importance of the unbiased biological pathway profiling approach to assess for novel mechanisms when results are difficult to interpret. When we found that the caspase inhibitor Ac-DEVD-CHO was effective in young but not aging mice, the reason was not immediately apparent. We turned to microarray analysis to explore potential unexpected pathways at work in the aging heart post MI. We found that not only was there more caspase 3 and 7 transcription, meaning more available to become activated in the cytoplasm, but also that there was activation of the Map3K1/MapK10 pathway that was not apparent in the young mice. Thus, the weight-based dose of caspase inhibitor that is effective in young mice may not be enough to inhibit the greater amount of caspase in the aging mice. Higher doses of this agent may be required and future studies are warranted to assess this. Furthermore, the upregulation of Map3K1/MapK10 pathway that is only seen in the aging mice may be partly responsible for the greater levels of apoptosis and the resistance to caspase inhibition. It is enticing to speculate that dual inhibition of the Map3K1/MapK10 and caspase pathways may be effective in preventing apoptosis in the aging infarcted heart, however this remains to be tested in future studies.

In summary, following MI we demonstrate an age-dependent increase cardiomyocyte apoptosis, and alterations in gene expression profile, which may contribute to the increase in post-infarction mortality with aging.

NIH-PA Author Manuscript

NIH-PA Author Manuscript

NIH-PA Author Manuscript

Supplementary Material

Refer to Web version on PubMed Central for supplementary material.

Acknowledgments

The microarray analyses were performed at the UCSF Gladstone Institute Genomics Core Facility and the analysis was performed by the UCSF Gladstone Bioinformatics Core Facility.

Funding

This study was funded by grants from the NIH K08HL090915 (AJB) and the Ellison Medical Foundation (AJB).

References

1. National Heart Lung and Blood Institute. Incidence and Prevalence: 2006 Chart Book on Cardiovascular and Lung Diseases: National Institutes of Health.
2. Ezekowitz JA, Kaul P, Bakal JA, Armstrong PW, Welsh RC, McAlister FA. Declining In-Hospital Mortality and Increasing Heart Failure Incidence in Elderly Patients With First Myocardial Infarction. Journal of the American College of Cardiology. 2009; 53:13–20. [PubMed: 19118718]
3. Maggioni AA, Maseri A, Fresco C, et al. Age-Related Increase in Mortality among Patients with First Myocardial Infarctions Treated with Thrombolysis. New England Journal of Medicine. 1993; 329:1442–1448. [PubMed: 8413454]
4. Shih H, Lee B, Lee RJ, Boyle AJ. The Aging Heart and Post-Infarction Left Ventricular Remodeling. Journal of the American College of Cardiology. 2011; 57:9–17. [PubMed: 21185495]
5. Liu P, Xu B, Cavalieri TA, Hock CE. Age-related difference in myocardial function and inflammation in a rat model of myocardial ischemia-reperfusion. Cardiovascular Research. 2002; 56:443–453. [PubMed: 12445885]
6. Lehrke S, Mazhari R, Durand DJ, et al. Aging Impairs the Beneficial Effect of Granulocyte Colony-Stimulating Factor and Stem Cell Factor on Post-Myocardial Infarction Remodeling. Circulation Research. 2006; 99:553–560. [PubMed: 16873716]
7. Boyle AJ, Shih H, Hwang J, et al. Cardiomyopathy of Aging in the Mammalian Heart is Characterized by Myocardial Hypertrophy, Fibrosis and a Predisposition Towards Cardiomyocyte Apoptosis and Autophagy. Experimental Gerontology. 2011; 46:549–559. [PubMed: 21377520]
8. Yeghiazarians Y, Zhang Y, Prasad M, et al. Injection of Bone Marrow Cell Extract Into Infarcted Hearts Results in Functional Improvement Comparable to Intact Cell Therapy. Molecular Therapy. 2009; 17:1250–1256. [PubMed: 19384293]
9. Zhang Y, Sievers RE, Prasad M, et al. Timing of bone marrow cell therapy is more important than repeated injections after myocardial infarction. Cardiovascular Pathology. 2011; 20:204–212. [PubMed: 20667749]
10. Dahlquist KD, Salomonis N, Vranizan K, Lawlor SC, Conklin BR. GenMAPP, a new tool for viewing and analyzing microarray data on biological pathways. Nature Genetics. 2002; 31:19–20. [PubMed: 11984561]
11. Salomonis N, Hanspers K, Zambon A, et al. GenMAPP 2: new features and resources for pathway analysis. BMC Bioinformatics. 2007; 8:217. [PubMed: 17588266]
12. Gentleman R, Carey V, Bates D, et al. Bioconductor: open software development for computational biology and bioinformatics. Genome Biology. 2004; 5:R80. [PubMed: 15461798]
13. Smyth GK. Linear models and empirical Bayes methods for assessing differential expression in microarray experiments. Statistical Applications in Genetics and Molecular Biology. 2004; 3:1. Article 3.
14. Gould KE, Taffet GE, Michael LH, et al. Heart failure and greater infarct expansion in middle-aged mice: a relevant model for postinfarction failure. American Journal of Physiology - Heart and Circulatory Physiology. 2002; 282:H615–H621. [PubMed: 11788410]
15. Bujak M, Kweon HJ, Chatila K, Li N, Taffet G, Frangogiannis NG. Aging-Related Defects Are Associated With Adverse Cardiac Remodeling in a Mouse Model of Reperfused Myocardial

NIH-PA Author Manuscript

NIH-PA Author Manuscript

NIH-PA Author Manuscript

Infarction. Journal of the American College of Cardiology. 2008; 51:1384–1392. [PubMed: 18387441]

16. Deten A, Marx G, Briest W, Christian Volz H, Zimmer H-G. Heart function and molecular biological parameters are comparable in young adult and aged rats after chronic myocardial infarction. Cardiovascular Research. 2005; 66:364–373. [PubMed: 15820205]
17. Yuan R, Tsaih S-W, Petkova SB, et al. Aging in inbred strains of mice: study design and interim report on median lifespans and circulating IGF1 levels. Aging Cell. 2009; 8:277–287. [PubMed: 19627267]
18. Jugdutt BI, Jelani A. Aging and Defective Healing, Adverse Remodeling, and Blunted Post-Conditioning in the Reperfused Wounded Heart. Journal of the American College of Cardiology. 2008; 51:1399–1403. [PubMed: 18387443]
19. Boyle AJ, Schuster M, Witkowski P, et al. Additive effects of endothelial progenitor cells combined with ACE inhibition and beta-blockade on left ventricular function following acute myocardial infarction. J Renin Angiotensin Aldosterone Syst. 2005; 6:33–37. [PubMed: 16088849]
20. Yeghiazarians Y, Gaur M, Zhang Y, et al. Myocardial Improvement with Human Embryonic Stem Cell-Derived Cardiomyocytes Enriched by p38MAPK Inhibition. Cytotherapy. 2012; 14:223–231. [PubMed: 22040108]
21. Yeghiazarians Y, Khan M, Angeli FS, et al. Cytokine Combination Therapy With Long-Acting Erythropoietin and Granulocyte Colony Stimulating Factor Improves Cardiac Function But is Not Superior Than Monotherapy in a Mouse Model of Acute Myocardial Infarction. Journal of cardiac failure. 2010; 16:669–678. [PubMed: 20670846]
22. Hatzistergos KE, Quevedo H, Oskouei BN, et al. Bone Marrow Mesenchymal Stem Cells Stimulate Cardiac Stem Cell Proliferation and Differentiation. Circulation Research. 2010; 107:913–922. [PubMed: 20671238]
23. Ye J, Boyle AJ, Shih H, et al. Sca-1+ Cardiosphere-Derived Cells Are Enriched for Isl1-Expressing Cardiac Precursors and Improve Cardiac Function after Myocardial Injury. PLoS One. 2012; 7:e30329. [PubMed: 22272337]
24. Ye J, Hom DS, Hwang J, Yeghiazarians Y, Lee RJ, Boyle AJ. Aging Impairs The Proliferative Capacity of Cardiospheres, Cardiac Progenitor Cells and Cardiac Fibroblasts: Implications for Cell Therapy. Journal of Clinical Medicine. 2013 In Press.

NIH-PA Author Manuscript
NIH-PA Author Manuscript
NIH-PA Author Manuscript

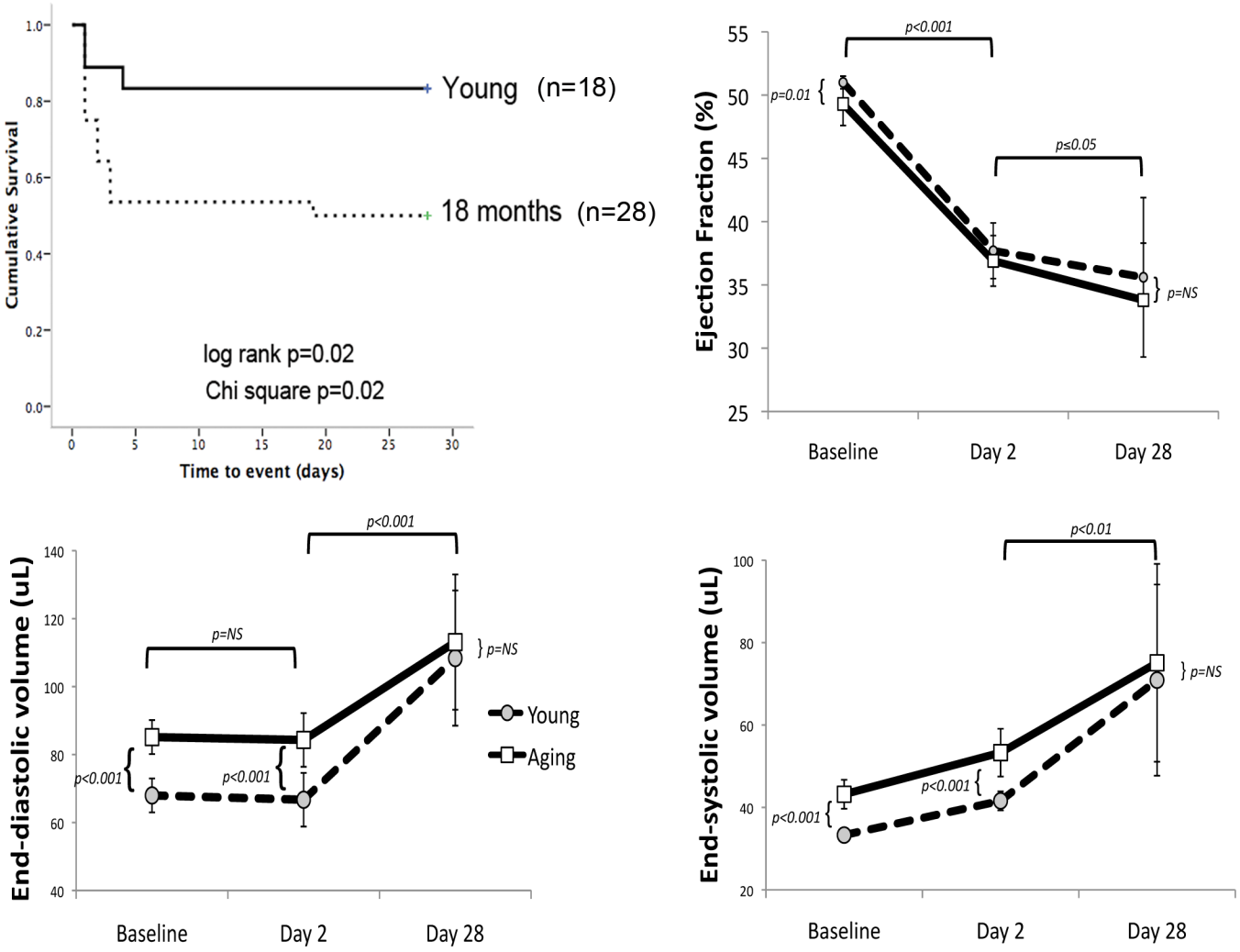

Figure 1. Mortality and Remodeling Following MI with Aging

Kaplan Meier curve demonstrates that survival following MI is dependent on age. At age 18 months, mortality significantly increases to approximately 50%. echocardiography demonstrates a greater degree of post-infarction left ventricular remodeling in the young mice. The smaller LV cavities in young mice at baseline dilate more than the aging, resulting in final LV volumes and ejection fractions indistinguishable at Day 28 post-MI.

NIH-PA Author Manuscript

NIH-PA Author Manuscript

NIH-PA Author Manuscript

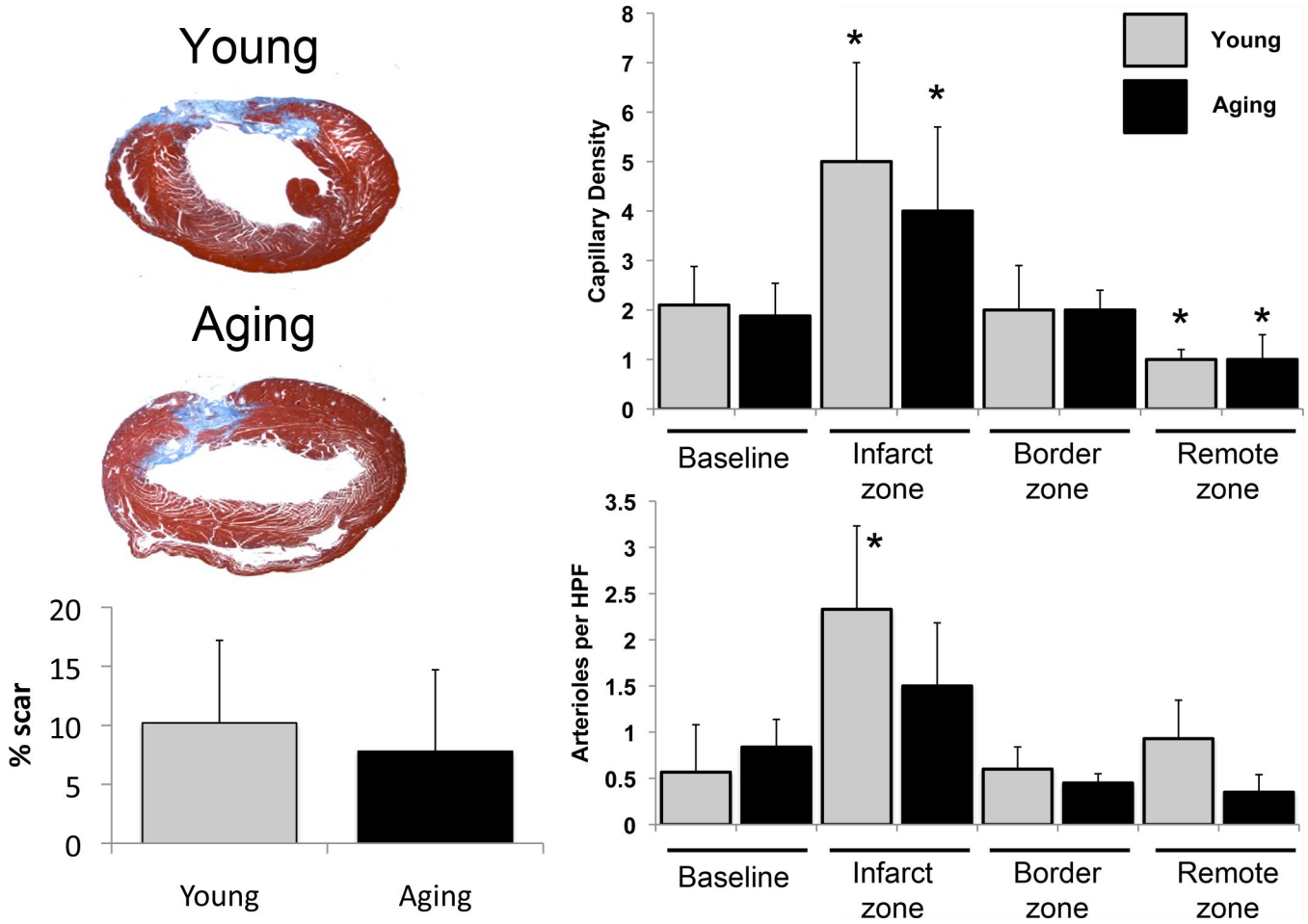

Figure 2. Age Does Not Affect Infarct Size or Vascularity in Survivors of MI

In mice surviving to day 28 post MI, there is no difference in infarct scar size between young and aging mice. Following MI, there is an increase in vascular density in the infarct zone in both young and aging mice. There is no difference in capillary or arteriole density between age groups in any region of the heart. * $p<0.05$

NIH-PA Author Manuscript

NIH-PA Author Manuscript

NIH-PA Author Manuscript

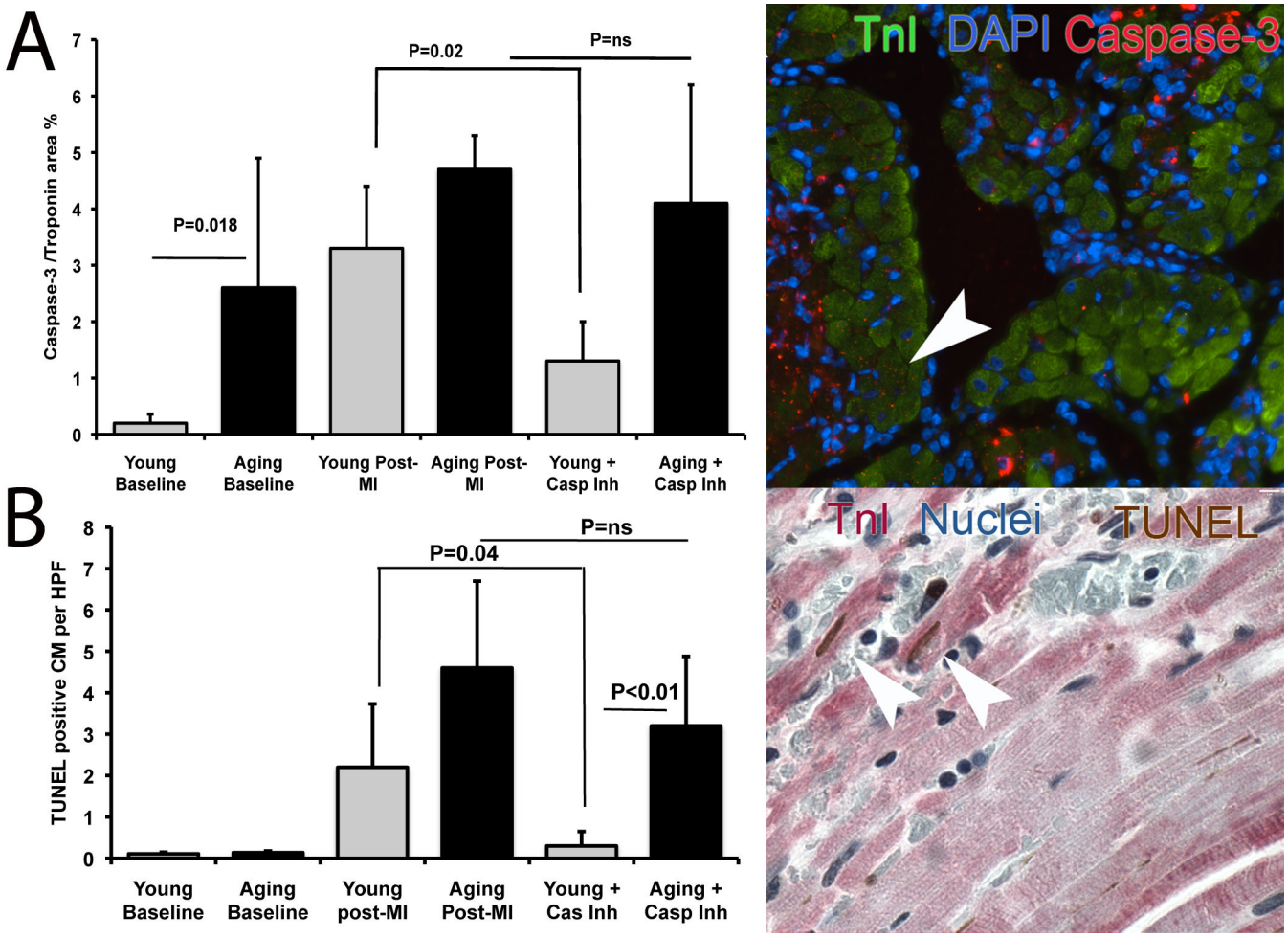

Figure 3. Aging Mice Have Increased Apoptosis and are Resistant to Anti-Apoptotic Therapy After MI

Because the pro-apoptotic gene profile in the left ventricle may be due to cell types other than cardiomyocytes, we performed immunohistochemistry to determine the level of apoptosis in cardiomyocytes. Following MI, there is an increase in cardiomyocyte expression of activate caspase-3 (A) and TUNEL staining demonstrates a corresponding increase in cardiomyocyte apoptosis in the infarct borderzone (B). With caspase inhibition, young mice exhibit reduction in the expression of active caspase-3 and in the number of apoptotic cardiomyocytes. However, aging mice are resistant to caspase inhibition. There is no reduction in either caspase expression (A) or the number of apoptotic cardiomyocytes (B) in aging mice.

NIH-PA Author Manuscript
NIH-PA Author Manuscript
NIH-PA Author Manuscript

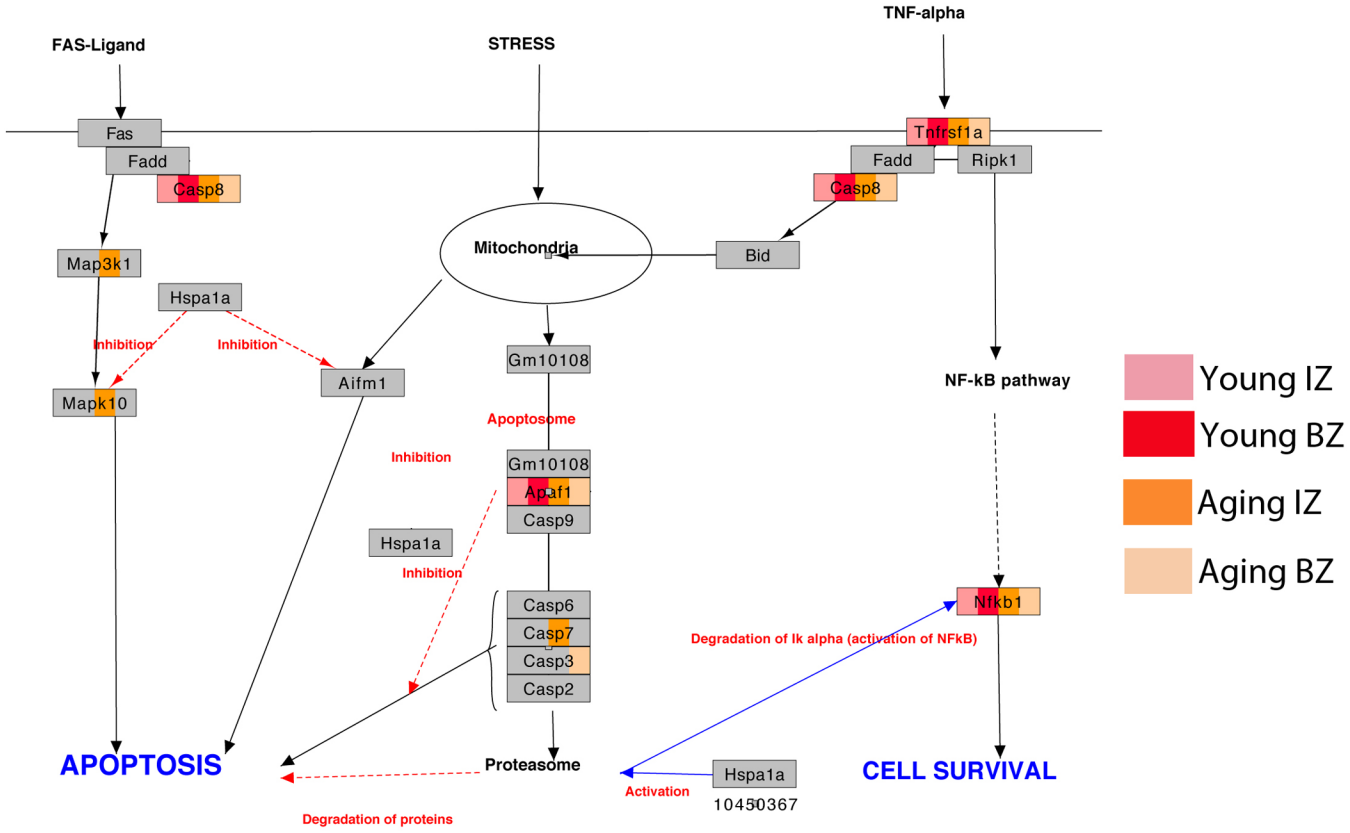

Figure 4. MI Induces Cardiomyocyte Apoptosis via Caspase-Dependent and Independent Mechanisms

Using GenMAPP software, we explored gene pathways that are known to mediate apoptosis. The pathway depicted is publicly available from Wikipathways.org via the GenMAPP program. Grey boxes indicate there is no change in expression of that gene following MI compared to baseline, colored boxes are significantly upregulated > 1.5-fold. Both young (red colored boxes) and aging mice (orange boxes) demonstrated upregulation of caspase 8 and Apaf1, as well as the protective NFkB pathway in the infarct and borderzone. However, the caspase 3 and 7 pathway, and the Map3K1 and MapK10 pathways demonstrate differential regulation, being upregulated in the aging mice but not the young.

NIH-PA Author Manuscript
NIH-PA Author Manuscript
NIH-PA Author Manuscript

Table 1

Echocardiographic and clinical data

	Young	Aging	p value
Heart weight (mg)			
Baseline	94.7±10.3	116.7±12.7	0.21
Day 28	137.5±12.2*	133.2±54.2	0.81
Body weight (g)			
Baseline	22.7±0.7	37.5±5.8	< 0.001
Day 2	20.8±0.9*	34.9±5.3	< 0.001
Day 28	25.9±1.4*#	34.3±4.4	< 0.001
Heart wt : body wt ratio			
Day 28	4.65±0.46	3.92±2.1	0.26
LVEDV (uL)			
Baseline	68.0±2.6	85.1±5.0	< 0.001
Day 2	66.7±3.6	84.3±8.0	< 0.001
Day 28	108.4±26.1*#	113.1±20.0*#	0.69
LVESV (uL)			
Baseline	33.3±1.1	43.2±3.5	< 0.001
Day 2	41.6±2.3	53.3±5.8	< 0.001
Day 28	70.9±23.2*#	75.1±24.0*#	0.73
LVEF (%)			
Baseline	51.0±0.5	49.1±1.6	0.01
Day 2	37.7±2.2*	36.9±2.0*	0.45
Day 28	35.6±6.3*	33.8±4.5*	0.54

Clinical and echocardiographic variables. P-values compare young versus aging.

For comparisons within age groups across time-points,

* denotes p<0.05 vs baseline;

# denotes p<0.05 vs Day 2.

NIH-PA Author Manuscript

NIH-PA Author Manuscript

NIH-PA Author Manuscript

Table 2
Changes in gene expression following MI in young and aging mice

Microarray analysis demonstrated a large number of individual genes, Elite GO terms and biological Wikipathways that are differentially expressed after MI. Aging hearts had similar numbers of changes compared to young hearts.

	Infarct Zone	Border Zone	Remote Zone
Young Post MI v Baseline			
Individual genes *>2 fold change, p<0.001*	1099	1108	328
Reported Elite GO terms *>1.5 fold change, p<0.01*	290	236	281
WikiPathways *>1.5 fold change, p<0.01*	37	37	25
Aging Post MI v Baseline			
Individual genes *>2 fold change, p<0.001*	1541	1042	384
Reported Elite GO terms *>1.5 fold change, p<0.01*	205	238	202
WikiPathways *>1.5 fold change, p<0.01*	24	33	20